Online-Journals.org

iJOE International Journal of Online and Biomedical Engineering

iJOE | eISSN: 2626-8493 | Vol. 21 No. 7 (2025) | OPEN ACCESS

https://doi.org/10.3991/ijoe.v21i07.49805

PAPER

Development of an Advanced 4D Foot Shape Model from Multiple Acquisitions at Different Flexion Angles

Giulia Pascoletti[1], Talal Bin Irshad[1], Giuliana Baiamonte[2], Giordano Franceschini[1], Elisabetta Zanetti[1], Michele Calì[2] (✉)

[1]Department of Engineering, University of Perugia, Perugia, Italy

[2]Electric, Electronics and Computer Engineering Department, University of Catania, Catania, Italy

michele.cali@unict.it

ABSTRACT

A major challenge in constructing models of the human body or body parts stems from the fact that they are actually composed of several solid bodies articulated together. Consequently, 3D models must be parameterised with reference to joint angles: scans of the foot taken at different plantar/dorsal flexion angles were used in this study as a benchmark. The implemented methodology was based on the regression fitting of landmark trajectories obtained on a limited number of foot poses; these same landmarks were then used to guide 3D mesh morphing to predict foot geometry at different plantar/dorsal flexion angles. A careful optimisation of the methodology was performed to identify the optimal set of foot scans. The comparison between the actual foot shapes obtained by 3D laser scanning and the predicted shapes showed that the average error is at most 6.57 ± 2.74 mm. The methodology indications were finally drawn based on these error estimates. Further works will consider combined motions including flexion/extension, internal/external rotation, and foot inversion/eversion.

KEYWORDS

4D model, 3D laser scanner, mesh morphing, foot landmarks, shape prediction

1 INTRODUCTION

Nowadays, the digital acquisition of patient-specific anatomy has become an established methodology in the medical field and is considered a fundamental starting point for the subsequent design of 3D models of customised devices, especially when additive manufacturing techniques are involved in their production [1]. Three-dimensional printers, in fact, find application in many sectors such as automotive [2], soft robotics [3], construction [4], food printing [5] and textile engineering [6, 7], as they allow tailor-made products to be created and immediately placed on the market, exploring new designs and offering more customisation possibilities [8]. Various technologies are used to initiate this manufacturing process, each of which has specific indications and accuracies [9], and the most common are based on scanning objects or parts of

Pascoletti, G., Irshad, T.B., Baiamonte, G., Franceschini, G., Zanetti, E., Calì, M. (2025). Development of an Advanced 4D Foot Shape Model from Multiple Acquisitions at Different Flexion Angles. *International Journal of Online and Biomedical Engineering (iJOE)*, 21(7), pp. 125–137. https://doi.org/10.3991/ijoe.v21i07.49805

Article submitted 2024-04-23. Revision uploaded 2024-07-21. Final acceptance 2024-07-24.

© 2025 by the authors of this article. Published under CC-BY.

the human body by means of photogrammetry or scanners using lasers or structured light. Whenever the object of analysis is not a single bone, the shape is not actually unique, as it depends on the angles of the joints. In fact, any part of the body includes not only solid bodies (bones) but also soft tissues that undergo extensive deformations during relative movements. Therefore, differences in joint angles result in different shapes that cannot be obtained trivially by applying a given motion to a single portion of the total volume. In such cases, more than one 3D model is required if different poses are planned. For example, shoe design must consider the entire gait cycle through a 4D model in order to provide comfortable support during walking and running [9] or during lower limb rehabilitation [10]; similar considerations apply to the design of exoskeletons, where it is necessary to ensure a correct fit during all work operations [11]; recent technological developments of these wearable robotic devices have made significant progress over the last decade in several sectors, including industry and space [12, 13], as well as healthcare by offering a remarkable variety of solutions for walking assistance and rehabilitation [14]. Their mechanical design involves the creation of compliant mechanisms and structures that can influence the efficiency and effectiveness of the entire system, interacting with the user in terms of adaptability, safety, efficiency and comfort [15]. Indeed, in the healthcare sector, this technology can help reduce the clinical costs associated with caring for people with neurological disorders and/or age-related diseases [16]. Similar problems are also reported with regard to garment design, where sewing positions need to be optimised in relation to skin movements and stresses [17]. In fact, with the rapidly increasing demands for customisation of garments, the design of garments has attracted more and more attention in the field of intelligent computer-aided systems. It is possible to improve the quality and reliability of the product, facilitating the disassembly and regeneration of the same [18, 19]; or the 3D scanned data is used to estimate the dynamic tension lines of the skin on part of the leg and locally analyse the deformation of the epidermis [20]. In all these cases, the evolution of shape and volume as a function of time must be captured and properly considered. This can be achieved through stereophotogrammetric techniques that enable the acquisition of the functional information needed to address the clinical problems in rehabilitation medicine by quantitatively capturing body poses and movements; the paths of different markers are then recorded and used to transform the initial reference mesh [21, 22]. Alternatively, an articulated internal skeleton methodology can be used to guide surface deformations [23].

It is important to outline that a different approach is explored here, adapting the path of certain skin landmarks with analytical functions whose parameters are established based on a limited set of scanned poses.

Foot flexion/extension was used as a benchmark to establish the accuracy of this methodology in relation to the number and specific poses considered for curve fitting.

It is worth remarking that this approach could bring some important advantages, as it does not require the approximation of joint movements and the a priori determination of the position of the joint axes; at the same time, the experimental effort would be limited by the analysis of a low number of poses rather than an infinite number as would, in theory, be necessary.

2 MATERIALS AND METHODS

The experimental setup has included three subjects without any prior foot pathologies. All subjects were properly informed about the aim of the study and signed an informed consent. The feet were scanned at five different flexion positions, moving from a 90° foot orientation with respect to the tibia to the fully extended configuration.

2.1 Equipment

The equipment used for the geometry acquisition comprised three Azure Kinect devices attached to a hollow ring so that they shared a common base plane. The devices were positioned 1.40 metres apart, forming a 120° angle in a daisy-chain configuration with their respective visual axes intersecting at the centre of the ring (see Figure 1). These, after an appropriate synchronisation to have one master device and two subordinate devices, allowed real-time acquisition of the desired area at surface level, avoiding errors and artefacts caused by the subject's difficulty in remaining still even for short periods of time. Each device had to be individually calibrated to a specific grid, and this operation took 1–2 minutes. The Kinect DK device was equipped with smaller and more powerful sensors, and the hardware included a 12-megapixel RGB colour camera, an inertial measurement unit (IMU), a circular array of seven microphones and a one-megapixel ToF depth camera. The latter can be set with a narrow field of view (Depth NFOV – Wide Field Of View) or with a wide field of view (Depth WFOV – Narrow Field Of View) and should ideally be positioned at the vertices of an equilateral triangle with sides of about 5 m in NFOV mode and about 3 m in WFOV mode to realise a capture area in order to obtain an adequate scan of the detected object with a resolution of about 320 × 288 and of about 512 × 512, respectively. It is well known that these devices are widely used for 3D pose and motion tracking [24, 25], calculating a set of 3D points that represent the body as a skeletal structure. The optimal configuration for foot scanning is that the ring base plane is perpendicular to the plantar surface of the foot; in addition, the foot should be approximately in the centre of the ring. Under these conditions, the accuracy of a shape scan should be less than 2 mm [26]. The result of the acquisition is a point cloud that was given as input to the RecFusion Pro software (ver. 2.3.0), producing an STL file with more than 150 000 elements, which is much more than required to maintain the 2 mm accuracy.

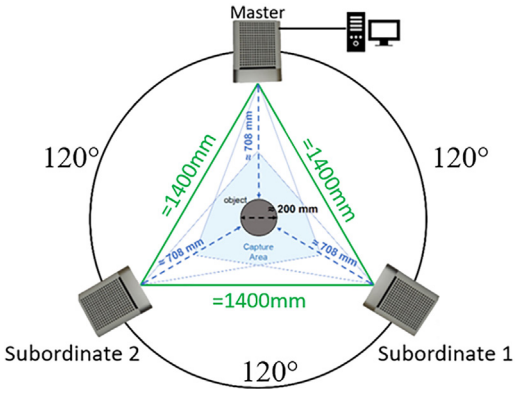

Fig. 1. Acquisition system configuration

2.2 Preliminary geometric processing

The STL files obtained at the end of the previous step were subjected to preliminary processing. This included merging all the toes without leaving any spaces in between in order to achieve greater consistency between the meshes of the same subject. Secondly, the meshes were imported into 3-Matic software (v. 20.0, Materialise Inc., Leuven, Belgium), and the calf axis was aligned to the global z-axis while the anteroposterior anatomical axis was aligned to the x-axis. The foot flexion angle α can be defined as the angle between the z-axis and the line tangent

to the two most prominent regions of the sole (see Figure 2) [27]. Finally, uniform remeshing resulted in a coarser mesh made of 10 000 elements, which still provides the required accuracy without incurring heavy computations.

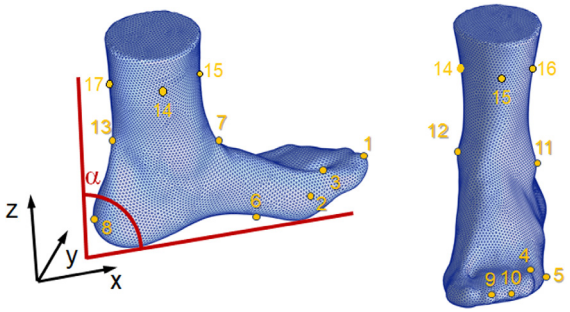

Fig. 2. Flexion angle definition and anatomical foot landmarks

2.3 Creation of isotopological meshes

Thirteen anatomical skin landmarks were identified on each foot (see Figure 2), based on the literature [28, 29] and taking into account the ISB (International Society of Biomechanics) indications [30]; four additional landmarks were added to also include the calf volume, reaching a total of 17 landmarks.

Mesh morphing from one foot, taken as a reference, to all the others was performed based on these landmarks and using a procedure based on radial basic morphing functions (RBF), implemented by a dedicated Matlab routine [31]: the new node positions were calculated on the basis of these functions.

This mesh control method, developed by [32, 33], was based on the RBF function interpolation to address the significant decrease in mesh quality and negative volume caused by mesh deformation. In the method, the volume mesh points with poor grid quality were adaptively selected and added to the RBF control point set according to the minimum distance criterion, and the displacements of the added points were determined by the weighted sum of those of the boundary surface points. Mesh deformation with the new control point set could effectively improve the local mesh.

In the next step, the nodes were projected onto the actual foot surface, and finally, a mesh smoothing was performed. This procedure resulted in all iso-topological meshes, consisting of 9636 nodes and 19268 elements, making possible one-to-one nodal matches among all feet (for any subject and any pose).

2.4 Landmarks path fitting

The total number of 3D meshes was equal to 15: 3 feet (subjects) per five poses (see Figure 3a). 10 meshes were used for landmark path fitting; the remaining five were used as control.

A number of preliminary operations were performed, such as a Procrustean analysis to centre and align all meshes against a common reference frame and scaling to eliminate distortions produced by feet of different sizes (see Figure 3b). The average shape was obtained as a result of the iterative Procrustes process (see Figure 3c).

The ten feet which were retained covered ten different flexion angles: 80°, 91°, 97°, 102°, 109°, 118°, 124°, 133°, 140°, and 151°. The regression fitting of landmark positions with respect to the flexion angle was tested for both linear and quadratic laws.

For each law, different sets of angles were included in the regression: the two extreme angles and one (for fitting on three data), two (for fitting on four data), and up to eight intermediate angles (for fitting over all ten input data).

In fact, the analysis was aimed not only at establishing the number of poses to be considered for accurate fitting but also at determining which poses were most significant and should be scanned to obtain the best regression law. Comparisons among different regression laws were performed by analysing the sum of the squared Euclidean distances between the 'true' and 'predicted' landmarks; this sum was extended to all nodes, poses and feet belonging to the control set.

2.5 From predicted landmarks position to predicted foot shape

With reference to each foot and each pose belonging to the control data set (5 poses), the average mesh was morphed according to the landmark position predicted by the interpolation law identified at the end of the previous step. The resulting meshes were scaled to recover the original foot size, and the root mean square error was computed over all nodes for each pose; finally, the results were averaged over all five samples.

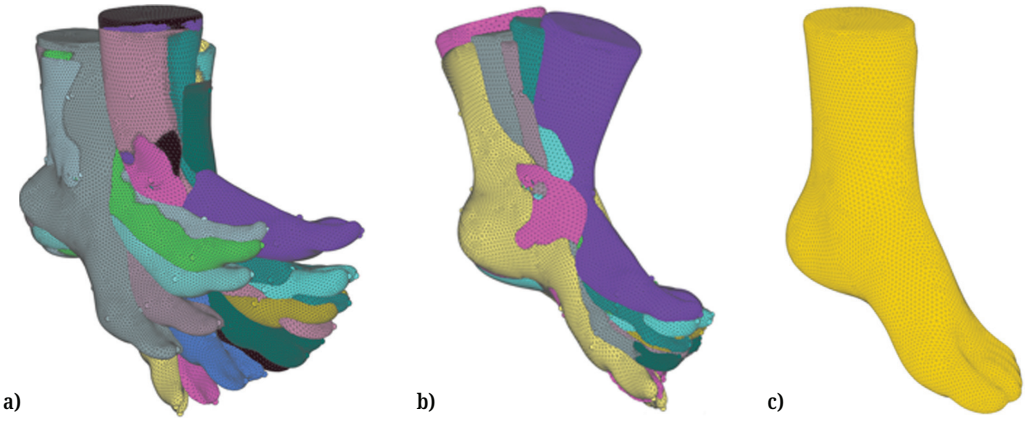

Fig. 3. (a) Original dataset; (b) dataset for fitting after Procrustes; (c) average shape

3 RESULTS

3.1 Regression fitting

Main results are reported in Table 1. For each fitting law, the combination of g angles that minimised the root mean square error (μRMS, g) is reported as a vector $\mathbf{C}_g$; g is the number of poses considered for landmark path fitting. As expected, the best fitting was obtained when all ten angles were considered, and quadratic laws generally provided a better fitting. According to the required accuracy, it was possible to identify the number of poses which must be considered as well as the best set of poses to be acquired, $\mathbf{C}_g$. Quadratic laws should be preferred unless 11.19 mm is considered as an acceptable accuracy.

3.2 Shape prediction on the control dataset

Shape prediction errors on the control dataset were assessed by performing the landmark path interpolation followed by mesh morphing. For this set of feet, the

interpolation of landmark displacements was performed referring to the quadratic law based on the four angles interpolation (g = 4; the third column in Table 1). The distance between the predicted position of landmarks and their actual position is reported in Figure 4, for both the x and z components and for the distance in the flexion plane (xz). The results are shown excluding the landmarks of the calf portion, the foot being the region of interest for the deviation analysis. Error distribution shows that the highest deviations are reported for landmarks 1, 9, 10 and 13, for which xz errors between 10 mm and 15 mm were found. For the landmarks associated to the toes (1, 9, 10), the highest deviation occurred in the x direction, while for the Achilles tendon region (13), the vertical displacement was the most critical. For all the other landmarks, the errors were kept below 10 mm, and the z deviations below 5 mm.

With reference to predicted shapes, Table 2 reports RMS errors computed over all poses and all nodes, while Figure 5 allows one to appreciate which areas and which poses are affected by the highest prediction errors.

Table 1. Mean errors obtained for the linear and quadratic fitting laws of landmark path versus foot flexion angles, given a number of poses considered for fitting g, and the results obtained for the best angle set are reported

g*	2	3	4	5	6	7	8	9	10
Linear									
$\mathbf{C}_g$**	80°	80°	80°	80°	80°	80°	80°	80°	80°
							91°	91°	91°
							97°	97°	97°
							102°	102°	102°
				109°	109°	109°		109°	109°
				118°	118°	118°			118°
			124°		124°	124°	124°	124°	124°
		133°	133°	133°		133°	133°	133°	133°
					140°	140°	140°	140°	140°
	151°	151°	151°	151°	151°	151°	151°	151°	151°
$\mu_{RMS,g}$*** [mm]	11.19	9.37	8.75	8.60	8.46	8.37	8.35	8.32	8.29
Quadratic									
$\mathbf{C}_g$**	–	80°	80°	80°	80°	80°	80°	80°	80°
							91°	91°	91°
							97°	97°	97°
							102°	102°	102°
			109°	109°	109°	109°		109°	109°
			118°	118°	118°	118°			118°
		124°			124°	124°	124°	124°	124°
						133°	133°	133°	133°
				140°	140°	140°	140°	140°	140°
		151°	151°	151°	151°	151°	151°	151°	151°
$\mu_{RMS,g}$*** [mm]		8.74	7.78	7.49	7.34	7.29	7.22	7.22	7.13

Notes: *g is the number of poses which was considered to set up the regression law (linear or quadratic) fitting landmark trajectories, **$\mathbf{C}_g$ is the vector of g poses which produces the best fitting, ***$\mu_{RMS,g}$ is the root mean square error when considering g poses.

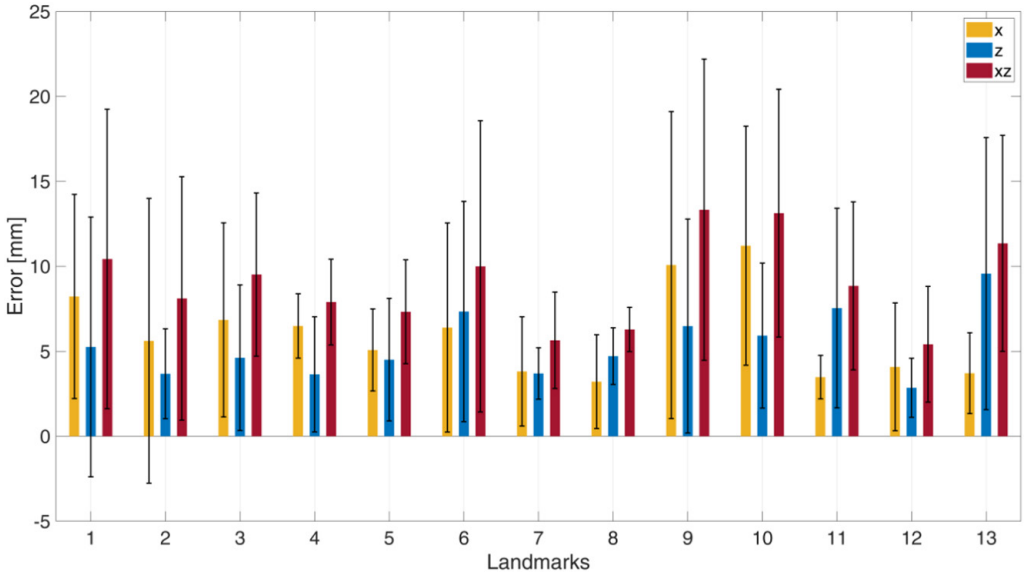

Fig. 4. Landmarks prediction error for x and z components and for the displacement in the flexion plane

Table 2. Mean and 90th percentile RMSE shape prediction for the control set

Foot	$\mu_{RMS} \pm \sigma_{RMS}$ [mm]	q90 [mm]
1	4.35 ± 1.76	6.56
2	3.16 ± 1.40	5.17
3	6.57 ± 2.74	10.28
4	5.06 ± 2.44	8.36
5	4.61 ± 2.25	7.40

4 RESULTS AND DISCUSSION

The results reported in Table 1 clearly show that it is more convenient to adopt a quadratic law for the regression of landmark path with respect to foot flexion. In addition, a set of four poses (g = 4) could be the most convenient one since the benefit of considering up to ten poses stays below 1 mm. These four poses should not be equally spaced between the two extreme positions (80° and 150°), since the range 110°–120° was found to be more critical. Following the procedure of quadratic landmark path fitting of four poses, errors on shape prediction keep, on average, below 5 mm, while 90% of nodes are affected by a distance error below 10.3 mm. These results were obtained on the control dataset, which was not considered to set up fitting laws; therefore, these results are representative of whatever foot at whatever position. The obtained errors are in line with those reported by authors who used other methodologies, such as the continuous scanning of landmarks (5.2 ± 2.0 mm) [34], while they are higher when compared to those of other authors who, instead, focused on foot shape variations produced by loading rather than foot flexion.

The deviation colour maps shown in Figure 5 agree with the results shown in Figure 4 on the prediction error of landmark positions in the flexion plane. Indeed, the highest deviations are located at the toes (landmarks 1, 9, and 10 in Figure 4) and are due to the variation of flexion angles of the respective joints. Another significant source of errors comes from ankle movements of internal/external rotation and/or

inversion/eversion. More refined models should track all these movements instead of just ankle flexion/extension; nonetheless, the methodology developed here represents a significant step forward compared to the production of a single 3D model, and it illustrated the accuracy which can be reached with a limited experimental effort. The results obtained on the control data set (refer to Table 2) were in agreement with those obtained on the sample set used to set up the regression laws (refer to Table 1, g = 4); this finding suggests that the sample set can be considered as representative of the entire population. Future work will be focused on the analysis of other movements: at this stage, the only flexion/extension was considered since this was the widest movement during gait [35].

The procedure set up here can be used for the design of garments and orthoses [36], and it has the advantage of covering a wide range of poses rather than a single one. In this way, fitting considerations can be more accurate, preventing the wearing of a particular foot/orthosis from resulting in a significant reduction in freedom of movements, shingles or abrasions.

5 CONCLUSIONS

In this work a novel approach for the prediction of foot geometry at different flexion angles was investigated. The main aim of the proposed methodology was to assess the prediction ability of a combined fitting-morphing model, using a limited number of poses as input. It was observed that, being able to reproduce the foot shape at any angle, only four feet scanned poses represent a significant benefit, as the burden resulting from continuous acquisition is significantly reduced. As expected, this implies higher errors; therefore, it should be carefully discussed according to the aim of the 3D reconstruction and the required accuracy.

A significant improvement might come from introducing further independent variables such as metacarpal joint flexion angle and hallux flexion angle; in fact, the landmarks which were affected by the highest errors were located on the metacarpus or at the hallux tip, and they got higher as the metacarpal joint angle grew, especially with reference to the z-axis position. The methodology could be profitably extended to the analysis of other movements such as foot inversion/eversion and internal/external rotation.

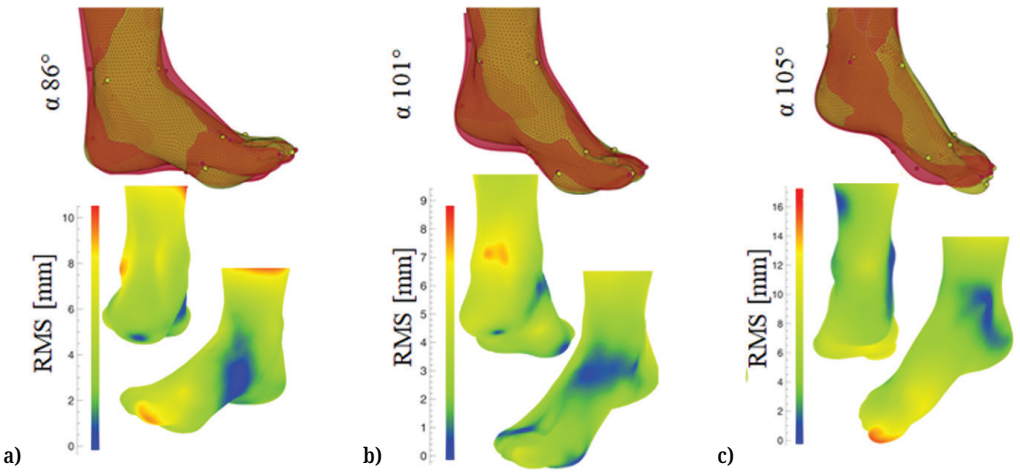

Fig. 5. *(Continued)*

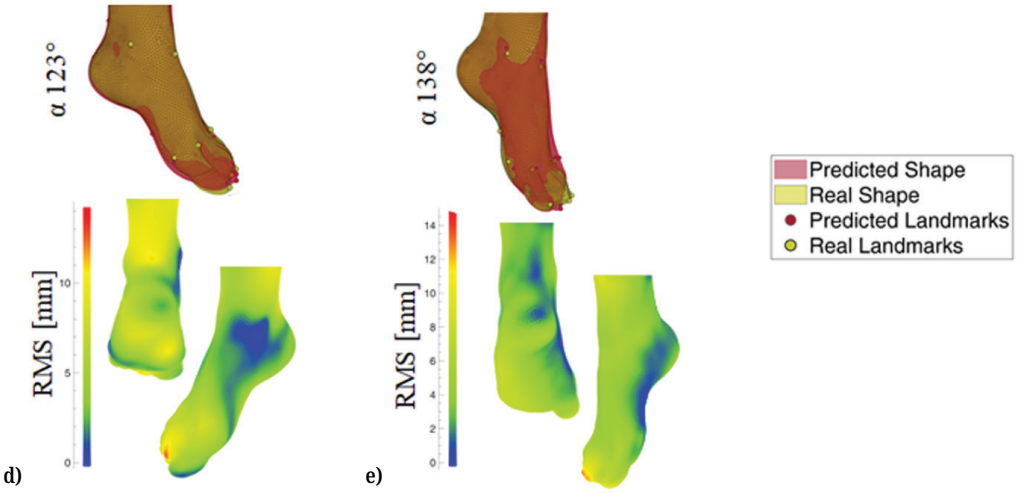

Fig. 5. Control dataset: shape predictions (upper part of each figure) and mean RMS error distribution (lower part of each figure) for foot #1 (a), foot #2 (b), foot #3 (c), foot #4 (d) and foot #5 (e)

6 CONFLICT OF INTEREST

The authors declare that the study was conducted in the absence of any commercial or financial relationships that could be construed as a potential conflict of interest.

7 AUTHOR CONTRIBUTIONS

GP and EZ have conceived the work; GB made experimental tests under the supervision of MC; GP and TBI processed the results; GP, EZ and MC have written the manuscript; all authors have discussed the results and reviewed the written text.

8 ACKNOWLEDGEMENTS

The authors thank Annacinzia Calì, Daniele Coco, Marta Coco, Rosario Coco, Pinella Porto, Sebastiano Granata and Giuseppe Laudani for their important contribution in the experimental tests.

9 FUNDING

This work was partially funded by the project “Modellazione Parametrica del corpo umano e dei suoi organi” funded by “Ricerca di Base 2021” of Università degli Studi di Perugia.

10 REFERENCES

[1] P. Volonghi, G. Baronio, and A. Signoroni, “3D scanning and geometry processing techniques for customised hand orthotics: An experimental assessment,” *Virtual and Physical Prototyping*, vol. 13, no. 2, pp. 105–116, 2018. https://doi.org/10.1080/17452759.2018.1426328

[2] M. R. Nichols, "How does the automotive industry benefit from 3D metal printing?" *Metal Powder Report*, vol. 74, no. 5, pp. 257–258, 2019. https://doi.org/10.1016/j.mprp.2019.07.002

[3] A. Zolfagharian, L. Durran, S. Gharaie, B. Rolfe, A. Kaynak, and M. Bodaghi, "4D printing soft robots guided by machine learning and finite element models," *Sensors and Actuators A: Physical*, vol. 328, p. 112774, 2021. https://doi.org/10.1016/j.sna.2021.112774

[4] Y. W. D. Tay, B. Panda, S. C. Paul, N. A. Noor Mohamed, M. J. Tan, and K. F. Leong, "3D printing trends in building and construction industry: A review," *Virtual and Physical Prototyping*, vol. 12, no. 3, pp. 261–276, 2017. https://doi.org/10.1080/17452759.2017.1326724

[5] Z. Liu, M. Zhang, B. Bhandari, and Y. Wang, "3D printing: Printing precision and application in food sector," *Trends in Food Science & Technology*, vol. 69, pp. 83–94, 2017. https://doi.org/10.1016/j.tifs.2017.08.018

[6] W. L. Ng, C. K. Chua, and Y. F. Shen, "Print me an organ! Why we are not there yet," *Progress in Polymer Science*, vol. 97, p. 101145, 2019. https://doi.org/10.1016/j.progpolymsci.2019.101145

[7] M. Askari, M. A. Naniz, M. Kouhi, A. Saberi, A. Zolfagharian, and M. Bodaghi, "Recent progress in extrusion 3D bioprinting of hydrogel biomaterials for tissue regeneration: A comprehensive review with focus on advanced fabrication techniques," *Biomaterials Science*, vol. 9, no. 3, pp. 535–573, 2021. https://doi.org/10.1039/D0BM00973C

[8] A. Zolfagharian, M. Lakhi, S. Ranjbar, and M. Bodaghi, "Custom shoe sole design and modeling toward 3D printing," *International Journal of Bioprinting*, vol. 7, no. 4, p. 396, 2021. https://doi.org/10.18063/ijb.v7i4.396

[9] H. B. Menz and D. R. Bonanno, "Footwear comfort: A systematic search and narrative synthesis of the literature," *Journal of Foot and Ankle Research*, vol. 14, p. 63, 2021. https://doi.org/10.1186/s13047-021-00500-9

[10] T. Spahiu, E. Piperi, A. Ehrmann, H. A. Almeida, R. M. Ascenso, and L. C. Vitorino, "3D printing: An innovative technology for customised shoe manufacturing," in *Progress in Digital and Physical Manufacturing: Proceedings of ProDPM'19*, in Lecture Notes in Mechanical Engineering, H. Almeida and J. Vasco, Eds., Springer, Cham, 2019, pp. 171–180. https://doi.org/10.1007/978-3-030-29041-2_22

[11] S. Dobashi, S. Kawaguchi, D. Ando, and K. Koyama, "Alternating work posture improves postprandial glucose response without reducing computer task performance in the early afternoon," *Physiology & Behavior*, vol. 237, p. 113431, 2021. https://doi.org/10.1016/j.physbeh.2021.113431

[12] J. Masood, J. Ortiz, J. Fernández, L. A. Mateos, and D. G. Caldwell, "Mechanical design and analysis of light weight hip joint parallel elastic actuator for industrial exoskeleton," in *2016 6th IEEE International Conference on Biomedical Robotics and Biomechatronics (BioRob)*, 2016, pp. 631–636. https://doi.org/10.1109/BIOROB.2016.7523696

[13] E. C. Lovasz *et al.*, "Design and control solutions for haptic elbow exoskeleton module used in space telerobotics," *Mechanism and Machine Theory*, vol. 107, pp. 384–398, 2017. https://doi.org/10.1016/j.mechmachtheory.2016.08.004

[14] M. Bortole *et al.*, "The H2 robotic exoskeleton for gait rehabilitation after stroke: Early findings from a clinical study," *Journal of NeuroEngineering and Rehabilitation*, vol. 12, pp. 1–14, 2015. https://doi.org/10.1186/s12984-015-0048-y

[15] M. Sanchez-Villamañan, J. Gonzalez-Vargas, D. Torricelli, J. C. Moreno, and J. L. Pons, "Compliant lower limb exoskeletons: A comprehensive review on mechanical design principles," *Journal of Neuroengineering and Rehabilitation*, vol. 16, pp. 1–16, 2019. https://doi.org/10.1186/s12984-019-0517-9

[16] P. T. Arun Jayaraman and W. Z. Rymer, "Exoskeletons for rehabilitation and personal mobility: Creating clinical evidence," in *Wearable Robotics: Challenges and Trends: Proceedings of the 2nd International Symposium on Wearable Robotics, WeRob2016*, J. González-Vargas, J. Ibáñez, J. Contreras-Vidal, H. van der Kooij, and J. Pons, Eds., vol. 16, Springer, Cham, 2016, pp. 21–24. https://doi.org/10.1007/978-3-319-46532-6_4

[17] J. Choi and K. Hong, "3D skin length deformation of lower body during knee joint flexion for the practical application of functional sportswear," *Applied Ergonomics*, vol. 48, pp. 186–201, 2015. https://doi.org/10.1016/j.apergo.2014.11.016

[18] J. M. Lu, M. J. J. Wang, C. W. Chen, and J. H. Wu, "The development of an intelligent system for customized clothing making," *Expert Systems with Applications*, vol. 37, no. 1, pp. 799–803, 2010. https://doi.org/10.1016/j.eswa.2009.05.089

[19] H. Zhou, Y. Xu, L. Wang, and Y. Chen, "A garment design method based on modularization," *Textile Research Journal*, vol. 86, no. 16, pp. 1710–1715, 2016. https://doi.org/10.1177/0040517515595027

[20] H. Seo, S. J. Kim, F. Cordier, J. Choi, and K. Hong, "Estimating dynamic skin tension lines in vivo using 3D scans," *Computer-Aided Design*, vol. 45, no. 2, pp. 551–555, 2013. https://doi.org/10.1016/j.cad.2012.10.044

[21] A. Menache, *Understanding Motion Capture for Computer Animation. 2nd ed.*, San Diego: Academic Press, 2011. https://doi.org/10.1016/C2009-0-62989-5

[22] M. D'Amico, E. Kinel, and P. Roncoletta, "Normative 3D opto-electronic stereophotogrammetric posture and spine morphology data in young healthy adult population," *PLoS One*, vol. 12, no. 6, p. e0179619, 2017. https://doi.org/10.1371/journal.pone.0179619

[23] L. Gao, Y. K. Lai, Q. X. Huang, and S. M. Hu, "A data-driven approach to realistic shape morphing," *Computer Graphics Forum*, vol. 32, pp. 449–457, 2013. https://doi.org/10.1111/cgf.12065

[24] T. M. Guess, R. Bliss, J. B. Hall, and A. M. Kiselica, "Comparison of Azure Kinect overground gait spatiotemporal parameters to marker based optical motion capture," *Gait & Posture*, vol. 96, pp. 130–136, 2022. https://doi.org/10.1016/j.gaitpost.2022.05.021

[25] C. Ferraris *et al.*, "Evaluation of arm swing features and asymmetry during gait in Parkinson's disease using the azure kinect sensor," *Sensors*, vol. 22, no. 16, p. 6282, 2022. https://doi.org/10.3390/s22166282

[26] G. Kurillo, E. Hemingway, M. L. Cheng, and L. Cheng, "Evaluating the accuracy of the azure kinect and kinect v2," *Sensors*, vol. 22, no. 7, p. 2469, 2022. https://doi.org/10.3390/s22072469

[27] D. M. Knapik, S. LaTulip, M. J. Salata, J. E. Voos, and R. W. Liu, "Impact of routine gastrocnemius stretching on ankle dorsiflexion flexibility and injury rates in high school basketball athletes," *Orthopaedic Journal of Sports Medicine*, vol. 7, no. 4, 2019. https://doi.org/10.1177/2325967119836774

[28] M. Xu, J. X. Li, Y. Hong, and L. Wang, "Foot morphology in Chinese adolescents aged between 13 to 18 years varies by gender and age," *Medical Science Monitor: International Medical Journal of Experimental and Clinical Research*, vol. 25, pp. 938–945, 2019. https://doi.org/10.12659/MSM.912947

[29] C. Price and C. Nester, "Foot dimensions and morphology in healthy weight, overweight and obese males," *Clinical Biomechanics*, vol. 37, pp. 125–130, 2016. https://doi.org/10.1016/j.clinbiomech.2016.07.003

[30] A. Leardini, J. Stebbins, H. Hillstrom, P. Caravaggi, K. Deschamps, and A. Arndt, "ISB recommendations for skin-marker-based multi-segment foot kinematics," *Journal of Biomechanics*, vol. 125, p. 110581, 2021. https://doi.org/10.1016/j.jbiomech.2021.110581

[31] G. Pascoletti, "Statistical shape modelling of the human mandible: 3D shape predictions based on external morphometric features," *International Journal on Interactive Design and Manufacturing (IJIDeM)*, vol. 16, pp. 1675–1693, 2022. https://doi.org/10.1007/s12008-022-00882-5

[32] M. Calì and R. Ambu, "A mesh morphing computational method for geometry optimization of assembled mechanical systems with flexible components," *International Journal on Interactive Design and Manufacturing (IJIDeM)*, vol. 16, no. 2, pp. 575–582, 2022. https://doi.org/10.1007/s12008-022-00850-z

[33] G. Pascoletti, M. Calì, C. Bignardi, P. Conti, and E. M. Zanetti, "Mandible morphing through principal components analysis," in *Design Tools and Methods in Industrial Engineering*, in Lecture Notes in Mech. Engineering, C. Rizzi, A. O. Andrisano, F. Leali, F. Gherardini, F. Pini, and A. Vergnano, Eds., Springer, Cham, 2020, pp. 15–23. https://doi.org/10.1007/978-3-030-31154-4_2

[34] R. W. Schuster, A. Cresswell, and L. Kelly, "Reliability and quality of statistical shape and deformation models constructed from optical foot scans," *Journal of Biomechanics*, vol. 115, p. 110137, 2021. https://doi.org/10.1016/j.jbiomech.2020.110137

[35] M. N. Anas, "An instrumented insole system for gait monitoring and analysis," *International Journal of Online Engineering*, vol. 10, no. 6, pp. 30–34, 2014. https://doi.org/10.3991/ijoe.v10i6.3971

[36] G. Govindaraj and A. S. A. Doss, "Evaluation of robotic ankle-foot orthosis with different actuators using simscape multibody for foot-drop patients," *International Journal of Online & Biomedical Engineering*, vol. 19, no. 10, pp. 156–168, 2023. https://doi.org/10.3991/ijoe.v19i10.40375

11 AUTHORS

Giulia Pascoletti is currently a post-doc researcher at the Department of Engineering at the University of Perugia. Her research interests cover the study of numerical models (multibody and finite element), with particular attention to industrial case studies and biomechanical applications (E-mail: giulia.pascoletti@unipg.it).

Talal Bin Irshad is a PhD student at the University of Perugia. He is involved in a project to set up a methodology for the design of patient-specific temporomandibular joints (E-mail: talalbinirshad@gmail.com).

Giuliana Baiamonte is a PhD student in Electric, Electronics and Computer Engineering Department at University of Catania. She received the Master Degree in Biomedical Engineering at the Bio-Medical Campus in Rome. Her main research interests are in biomechanics and in devices based on nanotechnology (E-mail: giuliana.baiamonte@unict.it).

Giordano Franceschini is a Full Professor in Industrial Bioengineering at the University of Perugia. He teaches Bioengineering at the Faculty of Engineering. His main research interests are related to human-vehicle interactions (E-mail: giordano.franceschini@unipg.it).

Elisabetta Zanetti is an Associate Professor in Industrial Bioengineering at the University of Perugia. She teaches Bioengineering at the Faculty of Medicine. Her main field of interests are orthopaedic and dental biomechanics (E-mail: elisabetta.zanetti@unipg.it).

Michele Calì is an Associate Professor in Electric, Electronics and Computer Engineering Department at University of Catania. He teaches Industrial Technical Drawing and his research interests include Reverse Engineering techniques, Rapid Prototyping techniques, CAD-CAE Modeling, Algorithms Processing, Computer Aided Tolerancing (CAT), Geometric and Structural Optimization particularly in mechanical and biomedical field (E-mail: michele.cali@unict.it).